[1] Chen Kai-nuo
Zhang Fu-guang[1]
Zhang Han[2]
Yin Yan-tao[1]
Du Guang-chuan[1]

Subsample Selection and Test Confidence Improvement in Equipment Accelerated Life Tests

Abstract: - In this study, the evaluation of equipment technical status was enhanced by refining the secondary indexes of the exiting status evaluation system based on equipment quality monitoring standards. An objective assessment of equipment technical status was achieved through this refinement. Additionally, a scientifically grounded sampling scheme was developed, and a multi-objective nonlinear integer programming model was established for accelerated life tests which yields an approximate optimal solution. To address instances where the conclusions from small sample tests do not meet the confidence level in classical reliability sampling theory, an improved dynamic time warping algorithm was employed. This algorithm measures the similarity between the original part and the spare part, demonstrating that the inclusion of spare part samples increases the sample size without altering the distribution of the original sample. Furthermore, in addressing the challenges of inheriting information from both new and old equipment, the mutual information method was employed to enhance the calculation of inheritance factors. These factors were then fused with multi-source test data, improving test confidence and offering valuable insights for enhancing confidence in small sample tests.

Keywords: Life extension test; Technical status evaluation; Index weight; Multi-objective multi-constraint sampling; Small sample test confidence

I. Introduction

Equipment storage and life extension projects involve organizing activities and processes related to equipment storage and technical life extension. The primary objective is to prolong the service life (storage life) of equipment. At present, many countries' standards do not require determining the storage life of equipment in a single instance; rather, they extend it incrementally through one or more storage life extension projects. In the research phase of storage life extension, constrained by limited funding, time, and the necessity to maintain equipment readiness, it is impractical to sequentially test all in-service equipment.

The main process of an accelerated life test involves designing a scheme for the equipment's key components (e.g., engine, booster, pyrotechnical products, control and guidance system) according to the requirements for extending its service life. This is followed by conducting an accelerated life test on the components with a sampling method. Subsequent analysis of the accelerated life test data provides conclusions [1]. The primary goal of this type of test is to verify whether the remaining storage life of the equipment meets specified quantitative requirements under predefined conditions. Therefore, the scientifically sound selection of samples for the analysis is crucial for obtaining meaningful conclusions. Surprisingly, there is a dearth of relevant literature on this subject.

In engineering practice, subsamples are typically selected according to life extension experience, and the magnitude of equipment required to extend service life ranges from dozens to thousands. However, for equipment with an order of magnitude around 100, life extension tests generally involve selecting no fewer than three pieces. The recommended sample size is 5% of the number of objects slated for service life extension, but not exceeding 20 [2]. However, conclusions from such small sample tests often fall short of meeting confidence requirements under classical mathematical reliability sampling theory. Therefore, additional spare samples must be included in the testing process alongside historical model test data to augment the sample size. It is also worth noting that practical differences often exist in the environmental profiles of original samples and spare part samples [3]. Despite this, they are typically treated as equivalent products, potentially diminishing the confidence level of the test.

[1] Naval Aviation University Yantai 264001 China；

[2]Yantai Education Enrollment Examination Institute Yantai 264003 China

The rigorous validation of the sampling method in scientific research centered on extending equipment service life holds paramount importance in terms of fiscal savings, the efficient execution of equipment storage, and successful service life extension projects.

In the present study, the first step was to refine second-level indexes within the equipment technical status evaluation system. The weight of each index was determined by employing a combination of neural network and social network analysis, resulting in thus calculating a technical state score for each piece of equipment. Subsequently, the technical states of the equipment were categorized into three levels.

Following this, distinct multi-objective and multi-constrained nonlinear integer programming models, selected according to technical position surveys and accelerated life test samples, were established. An improved particle swarm algorithm was applied to solve these models. Given the lack of in-depth and systematic exploration of the environmental profile differences between original and spare samples, an improved dynamic time regularization algorithm was established. This algorithm facilitated the calculation of similarity between the samples, enabling quantitative assessment of the confidence relationship between spare samples and test conclusions.

Finally, in addressing the challenge of small sample test conclusions falling short of confidence requirements under classical mathematical reliability sampling theory, the mutual information measurement method was employed. This method yields calculations of the inheritance factor of new and old models. The inheritance factor was integrated with test data from historical models, expanding the sample size and raising the confidence level as a strategic solution to the limitations of small sample tests.

II. Related Works

Index weighting generally includes subjective, objective, or combinations of subjective-objective methods. The analytical hierarchy process (AHP) is a commonly used subjective weighting method which leverages mathematical and psychological principles to formulate and analyze complex decisions. First proposed by Saaty [4], AHP has been extensively studied and applied in multiple criteria decision making (MCDM) over the past two decades. Its main operations encompass hierarchy construction, priority analysis, and consistency verification [5], providing a framework to synthesize expert judgments, establish priorities between standards, and identify alternative solutions. However, AHP's reliance on subjective expert judgments raises concerns about potential distortions in decisions if these judgments are inaccurate or biased [6].

Objective weighting involves deriving weights directly from the original information of indexes through statistical methods. Principal component analysis, the variation coefficient method, and the entropy method are representative examples. Principal component analysis (PCA) weighting is a relatively straightforward weighting method, assuming that index correlations can be captured by linear combinations [7]. The process involves standardizing data, calculating covariance matrixes, determining the weights of principal components, and other related calculations. However, the practical application of PCA requires consideration of nonlinear relationships between indexes or special circumstances, which must be verified to align with actual situations [8].

The entropy weight method (EWM) measures value dispersion in decision-making, assigning higher weights to more differentiated indexes. Despite being less influenced by subjective factors than PCA, EWM is prone to the randomness of sample data, leading to varying weights with different samples. Zhu [9] suggests that an excess of zeros in EWM's standardized results can distort outcomes, resulting in overemphasized indexes and reduced actual differentiation. Furthermore, EWM neglects hierarchical discrimination in multi-index decisions, hindering its ability to accurately reflect the importance of index weights.

While the simple objective weighting method may not readily incorporate index correlations or specific circumstances, combining comprehensive trade-offs and evaluations with other methods in practical applications becomes imperative. This would ensure that decision-making needs and objectives are accurately reflected, acknowledging the inherent limitations of individual weighting techniques.

In the safety assessment of numerous parts of engineering equipment, the determination of weights tends to rely heavily on the subjective experience of experts, neglecting the objective requirements for evaluating index status. This oversight limits the adaptability of evaluation systems to the advancements in modern equipment health monitoring technology. In efforts to remedy this, Shen [10] introduced a pipeline disaster assessment index system

tailored to permafrost areas, proposing a comprehensive weight determination method based on improved fuzzy hierarchy, the entropy weight method, and the Lagrange algorithm. They established a fuzzy comprehensive model for the safety evaluation of permafrost pipelines, validating the rationality of their method through a comparison with traditional hierarchical analysis. However, subjective experience and opinions still play a role in this subjective-objective weighting method, posing a risk of deviation (particularly when subjective factors dominate). Moreover, it relies on objective data and information. Incomplete or low-quality data can impact the accuracy of weights and the reliability of the evaluation results.

Social network analysis (SNA) [11] is a more objective weight assignment method. SNA quantifies the importance of nodes and hierarchical indexes by calculating the network indexes of each node (e.g., degree centrality, closeness centrality, betweeness centrality). This quantification, based on the entire network structure, reflects the relative positions and roles of indexes in the network with minimal influence from individual subjective factors [12]. In addition, SNA can be applied to explore the influence of network structures or changes in node location on the overall network through simulation or statistical analyses, enhancing the scientific nature of weight assignment.

The PageRank algorithm, proposed by Google founder Larry Page [13][14], provides another objective approach to weight determination. It involves evaluating the importance of a web page based on the reference relationships of links in a directed graph representing the internet. The PageRank algorithm calculates the importance indexes, known as PageRank values, for each web page; these values aid in sorting search results, providing relevant and authoritative information [14]. While the PageRank algorithm has some limitations, scholars have proposed various optimization methods to address its original design constraints [15].

The particle swarm optimization (PSO) algorithm is mainly used to solve global or quasi-minimum values in nonlinear non-convex optimization problems. There have been few studies to date on problems involving discrete decision variables. Considering the prevalence of nonlinear integer programming in the engineering field, Chen [16] introduced a PSO algorithm based on genetic operators, which handles integer limitations by encoding solutions, which manages integer constraints by encoding solutions, utilizing optimal solutions from groups and individuals, and updating particles through crossover, variation, and selection. Numerical experiments validated the feasibility and effectiveness of this algorithm in solving large-scale problems. Sahoo [17] devised an efficient hybrid method based on the genetic algorithm and PSO algorithm to tackle nonlinear reliability optimization problems with mixed integers in series, series and parallel, and bridge systems. This method maximizes overall system reliability under the constraints of nonlinear resources, including cost, volume, and weight. Sun [18] proposed an improved PSO algorithm that expedites optimized convergence by linearly reducing inertial weights. An effective design method for searching spatial dimensions was simultaneously established to achieve satisfactory accuracy and reduce the number of iterations. Experiments demonstrated that this PSO algorithm can search for global optimal solutions highly effectively and that it has significant advantages compared to other scheduling algorithms.

Dynamic time warping (DTW) is an algorithm used to compare the similarity between two sequences [19] [20]. It disregards distortions and deformations on the timeline, aligning the two sequences in time for effective comparison. Guo et al. [20] introduced the dynamic search step SegrDTW algorithm, building on an improved DTW algorithm. SegrDTW considers starting and stopping data constraints and the coupling relationship between a doorway path and vehicle trajectory. By establishing a spatial window for segment retrieval, the DTW algorithm's spatial complexity was effectively reduced while significantly enhancing the efficiency of abnormal electronic toll collection (ETC) data detection.

Mutual information (MI) is a concept utilized to measure the correlation between two random variables, characterizing the degree of dependency between them. It has been widely applied, particularly in feature selection, data compression, and pattern recognition fields [22].

Inspired by these previous studies, a systematic method for sample selection in equipment storage life extension projects was developed in the present study. Assuming a small number of samples, historical experimental data and spare part data were combined to improve test confidence. The framework of the proposed method is illustrated in Fig. 1.

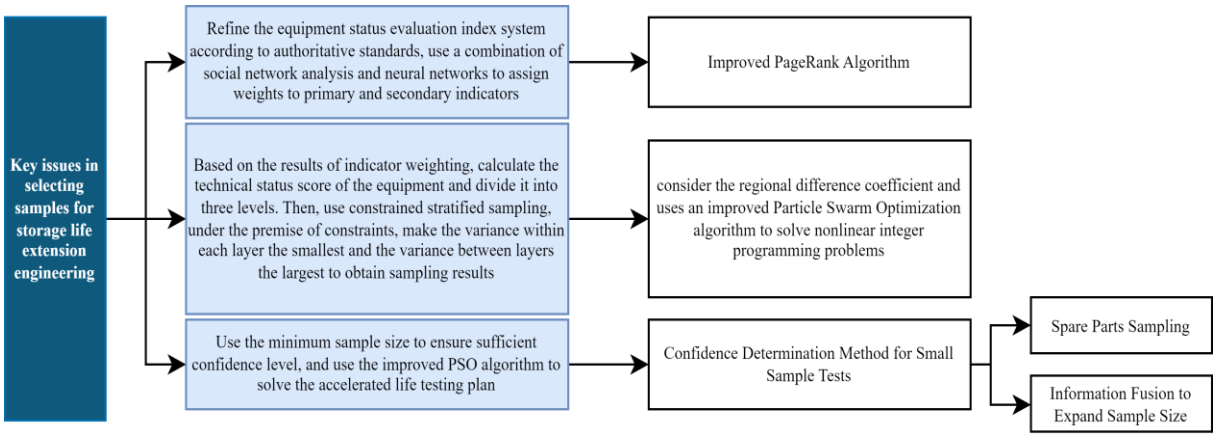

Fig. 1 Frame diagram: Flow and content of analysis

The main academic contributions of this paper can be summarized as follows.

1. In the comprehensive evaluation of equipment, an innovative approach is employed by integrating multilayer perceptron (MLP) with SNA to objectively and accurately determine index marks and weights. This method essentially leverages the robust learning capabilities of MLP and the network structure analysis proficiency of SNA to assess primary and secondary indexes of equipment scientifically and equitably.

2. A nonlinear integer programming model was established for the sampling process of life extension analysis, and an improved PSO algorithm was applied to solve the model. This yielded an approximate optimal solution under multiple constraints.

3. During equipment sample testing, instances may arise where the confidence level does not satisfy the criteria for classical reliability sampling. To address this, we integrated data from similar models and test data from spare samples. We utilized the mutual information solution inheritance factor and a dynamic time regularization (i.e., DTW) algorithm to calculate the similarity between original and spare part samples individually. By fusing multi-source test data, the confidence of test conclusions was improved while expanding the sample size.

III. Weighting of Equipment Technical Status Indexes, Sampling Model Solution Methodology

Based on an authoritative product quality monitoring standard, the primary indexes considered for evaluation include the product's service life, appearance, number of overhauls, performance, and service experience. Building upon this standard, secondary indexes of the comprehensive technical status evaluation index system for the product were established in this study. The specific technical indexes are listed in Table 1.

Table 1 Comprehensive evaluation index system for product technical status

Target layer	Factor layer	Index layer
Evaluation system of product status	A Service life	A1 Cumulative power-on time A2 Cumulative on-duty hours A3 Cumulative on-duty times A4 Cumulative storage time A5 Time beyond service life designated by instructions A6 Cumulative flight time

	B Appearance	B1 Surface shape (e.g., damage, deformation) B2 Surface paint B3 Surface corrosion B4 Aging of rubber products B5 Oil (liquid) leakage B6 Aging of cables B7 Gap size B8 Nameplate
	C Number of overhauls	C1 Cumulative number of failures C2 Cumulative repair duration C3 Longest singular repair time C4 Minimum failure interval C5 Average failure interval C6 Average fault repair time C7 Number of locations where failure occurred C8 Maximum number of failures in same location
	D Performance	D1 Whether technical parameters of mechanical products satisfy requirements D2 Whether technical parameters of electrical products satisfy requirements D3 Whether technical parameters of electronic products satisfy requirements D4 Whether technical parameters of optical products satisfy requirements D5 Whether technical parameters of oil (liquid) products satisfy requirements D6 Whether technical parameters of pyrotechnic products satisfy requirements
	E Service experience	E1 Temperature of service environment

	E2 Moisture content of service environment E3 Cumulative transportation mileage E4 Salt spray in service environment E5 Mold in service environment

As a method for examining social relations, SNA regards participants in society as nodes and their relationships as edges in a complex network that can be used to determine structural characteristics as well as the locations and roles of nodes. When analyzing social networks, individuals within the network (e.g., people, organizations, specific objects) are typically considered nodes while their relationships (e.g., business connections, knowledge transfer) are regarded as edges. By analyzing the distribution, connection patterns, and characteristics of these nodes and edges, a comprehensive understanding of the structure and dynamics of the network can be obtained. The characteristics of SNA can be summarized as follows.

1. It prioritizes relationships over attributes, concentrating on connections among nodes rather than the inherent characteristics of nodes.

2. It uses network theory and graph theory in analyzing a network's characteristics such as density and centrality.

3. It facilitates quantitative analysis based on mathematical and statistical tools for observing network characteristics.

4. It adopts a holistic view, not only analyzing individuals but also focusing on the overall network structure.

5. It emphasizes the importance of location, where the positions of individuals in the network influence their behavior.

Comprehensive evaluation indexes for technical product statuses are widely used to measure the importance, influence, or other specific attributes of individuals experimentally. The PageRank algorithm is crucial for enhancing accuracy and objectivity in this process. Initially designed for web page ranking, the PageRank algorithm assigns a relative weight value to each node based on relationships within the network, effectively measuring the importance of each node. By applying the PageRank algorithm, a precise and objective numerical rating can be assigned to comprehensive status evaluation indexes, ensuring an accurate reflection of their actual roles in product evaluations.

The original PageRank algorithm has practical limitations in terms of network analysis research. Firstly, it treats all links in the network as equal in weight, neglecting potential variations in quality between different links. Specific links may differ in quality or importance according to their sources, goals, or interaction dynamics. The uniform weighting of all links may result in overestimations of certain low-influence indexes or underestimations of high-influence indexes. This oversight can significantly deviate the results from the actual network structure and dynamics.

Secondly, the original algorithm does not consider thematic correlations between network nodes. In many practical applications, the theme or category of nodes serves as an important factor influencing the importance of the links between them. For example, even if an index contains key information, its link to seemingly unrelated content could lead to an overestimation of this link's importance, thereby impacting the final network analysis results. Moreover, the original algorithm encounters challenges in processing circular links within the network (e.g., index A linking to B while B links back to A). Circular links are prevalent in many actual networks, and if not managed properly, can destabilize the algorithm and even render inaccurate the final results of network analysis.

An enhanced PageRank algorithm was devised in this study to address these shortcomings. This enhanced version incorporates key improvements and optimizations in network link processing, considers the relevance of node themes, and manages circular links so as to analyze network structures and dynamics more accurately and stably. The specific improvements are as follows.

1. In the PageRank algorithm, the initial weight configuration significantly influences trajectories within the network. Establishing a suitable distribution for initial weights enhances the results to better align with the given requirements. Neural network training was utilized in this study to determine the initial weight w_{int} of each index, a

pivotal step in implementing the enhanced PageRank algorithm. Specifically, we used a fully connected neural network with a three-layer structure comprising an input layer, hidden layer, and output layer. The input layer's dimension was set to 34, corresponding to the 34 primary (first-level) and secondary (second-level) indexes in the dataset. The hidden layer dimension was set to 128, allowing the network to learn the complex nonlinear relationships between indexes. The dimension of the output layer was set to 5, generating a 5-dimensional vector corresponding to the initial weight w_{int}.

The training process of the neural network can be expressed in the following mathematical form: $w_{int} = f_\theta(x)$, where $f_\theta(x)$ is the function of the neural network, x is the first- and second-level index of the input, and θ is the parameter of the neural network to-be-learned through training.

The goal of training is to find a parameter set θ which ensures that the network's output w_{int} satisfies the relevant requirements. We trained the neural network for 500 rounds, continuously updating and optimizing θ to target these requirements as per the network output w_{int}. After training, an appropriate initial weight configuration was obtained under the current network structure, providing strong support for the initial weight settings of the PageRank algorithm.

2. We also introduced a "random walk". Personalized PageRank, an extension of the original PageRank algorithm which introduces personalized features, is a powerful tool for network analysis. This feature allowed us to control the network's walk behavior more flexibly to better meet the needs of specific tasks.

Consider a network with seven nodes: A, B, C, D, E, F, and G. Nodes A-D are directly connected to the starting node while nodes E-G are not directly connected. Personalized PageRank permits the specification of the starting probability for each node by defining an initial personalized vector. For instance, setting an initial vector as [0.1,0.1,0.1,0.1,0.1] assigns an equal probability to all nodes, resulting in uniformly random behavior for the random walker.

To emphasize the influence of the starting node, the personalized vector can be adjusted. For example, altering the vector to [0.3, 0.3, 0.3, 0.05, 0.05, 0.05, 0.05, 0.05] places higher probabilities on nodes directly connected to the starting node. This not only initiates the algorithm from specific nodes but also better reflects the importance of these nodes in the network. It also enhances the stability of stratified sampling. Despite these changes in initial weights, the results of Personalized PageRank consistently converge to a stable state distribution, offering a reliable method for hierarchical weighting. In this new vector, the probability of nodes directly connected to the starting node (A, B, C, D) is elevated while the probability of nodes indirectly connected or not connected to the starting node (E, F, G) is reduced. This implies that random walkers are more inclined to access nodes directly connected to the starting node.

The ability to control random walker behavior is beneficial for various network analysis tasks, including community discovery and node classification. In this study, we used this method to guide the PageRank algorithm to achieve more accurate weighting of primary and secondary indexes.

We used a cross-stratified sampling strategy in this study, carefully accounting for the two variables: the technical status and storage location of each sample. The dataset contains a total of 100 samples, each of which is characterized by a technical status (divided into primary, secondary, and tertiary indexes) and a storage location (divided into locations A, B, and C).

We first divided the samples into three layers based on their technical statuses, then further divided them into three sub-layers in each layer according to their storage locations. The final index weights are shown in Table 2.

Table 2 Final comprehensive evaluation index for product technical status

A	0.2	A1	0.05
		A2	0.04
		A3	0.04
		A4	0.03
		A5	0.02
		A6	0.02

B	0.15	B1	0.03
		B2	0.02
		B3	0.03
		B4	0.02
		B5	0.02
		B6	0.01
		B7	0.01
		B8	0.01
C	0.1	C1	0.02
		C2	0.02
		C3	0.02
		C4	0.01
		C5	0.01
		C6	0.01
		C7	0.005
		C8	0.005
D	0.25	D1	0.08
		D2	0.06
		D3	0.05
		D4	0.04
		D5	0.02
		D6	0.01
E	0.3	E1	0.12
		E2	0.08
		E3	0.06
		E4	0.02
		E5	0.02

Combining the final indexes in Table 2 with cross-stratified sampling allowed us to determine the final classification results, as discussed below.

Table 3 Stratified calculation results

tech_status	loc	Sample
status1	locationA	5, 6, 10, 12, 14, 15, 17, 18, 19, 20, 24, 25, 26, 27, 28, 29, 32, 34, 35, 38, 39, 40
	locationB	41, 42, 43, 44, 45, 46, 49, 54, 59, 60, 61, 62, 64, 66, 67, 70, 71, 75, 77, 80, 81, 82
	locationC	83, 84, 85, 86, 90, 91, 93, 94, 96, 98, 99
status2	locationA	1, 3, 4, 7, 8, 9, 11, 13, 16, 21, 22, 23, 30, 33
	locationB	37, 47, 48, 50, 51, 52, 55, 58, 63, 65, 69, 72, 73

	locationC	76, 78, 79, 87, 88, 89, 92, 95, 97, 100
	locationA	2, 31, 36
status3	locationB	53, 56, 57
	locationC	68, 74

For the test sampling model, ensuring a reasonable confidence level necessitates the use of the minimum sample. Assuming a result [passed, not passed], a binomial distribution with a probability of success p and confidence constraints need to be introduced to determine the required sample size n:

$$n \geq \frac{4Z^2 \cdot p \cdot (1-p)}{E^2}, \tag{1}$$

where Z is the z-score of the confidence interval (for example, at 95 % confidence, $Z \approx 1.96$), $\boldsymbol{p}$ is the probability of success in the sample, the empirical value of which is about 0.98 as per the historical data; $\boldsymbol{E}$ is the allowable error, generally 0.05 or 0.1.

The specific process involves assuming the probability of success p in the sample test results, extracting n independent samples from this distribution. And applying the law of large numbers and the central limit theorem. The confidence level in this case is $1 - \alpha$ (usually 95%), the sample mean $\bar{X}$ equals p, and the standard deviation is $\sqrt{\frac{p(1-p)}{n}}$. When n is sufficiently large, the probability that the normal distribution contains $1 - \alpha$ is between $-Z$ and Z.

In the case of $1 - \alpha = 0.95, Z \approx 1.96$. For the normal distribution, the 95% confidence interval can be expressed as follows:

$$\bar{X} \pm Z \cdot \sigma, \tag{2}$$

where $\bar{X}$ is the sample mean, σ is the standard deviation of the sample, and Z is the z-score corresponding to the required confidence level. In our example, $\sigma = \sqrt{\frac{p(1-p)}{n}}$, therefore:

$$\bar{X} \pm Z \cdot \sqrt{\frac{p(1-p)}{n}}. \tag{3}$$

The width of the above interval should not exceed the allowable error E, that is:

$$2Z \cdot \sqrt{\frac{p(1-p)}{n}} \leq E. \tag{4}$$

Squaring both sides of the inequality simultaneously yields the following:

$$4Z^2 \cdot \frac{p(1-p)}{n} \leq E^2. \tag{5}$$

Finally, by solving this inequality, the expression *of* n is:

$$n \geq \frac{4Z^2 \cdot p \cdot (1-p)}{E^2}.$$

(6)

By summarizing the survey sampling model, the test sampling model was formulated as follows.

Objective function: $min\, z_{\square} = n_A + n_B + n_C$.

(7)

1. Confidence constraint：

$\sum n_i \geq \frac{4Z^2 \cdot p \cdot (1-p)}{E^2}$.

(8)

2.Time constraint: $max(\, 3n_A; 3n_B; 3n_C) \leq 30$.

(9)

3. Personnel constraint: $8n_A + 8n_B + 8n_C \leq 100$.

(10)

4. On-duty ready-for-use rate constraint:$\frac{n_A}{N_A} \leq 0.2$， $\frac{n_B}{N_B} \leq 0.2$， $\frac{n_C}{N_C} \leq 0.2$.

(11)

In the above, N_A is the total number of products in location A; N_B is the total number of products in location B; N_C is the total number of products in location C; n_A is the number of samples extracted from location A; n_B is the number of samples extracted from location B; n_C is the number of samples extracted from location C; and *z* is the total number of samples.

Given the complexity of nonlinear integer programming problems, the PSO algorithm was employed to find the approximate optimal solution. The PSO algorithm first randomly initializes the particle swarm within a designated solution space. The dimensions of the solution space are determined by the number of variables to be optimized (represented here as *D*, denoting the dimension of each particle). Each particle is assigned an initial position *x* and velocity *v*; a crucial aspect of the algorithm is the updated formula for velocity. This velocity update is directional, consequently influencing the solution.

The optimization process unfolds iteratively. In each iteration, each particle updates its spatial position and flight speed within the solution space by tracking two "extreme values": the particle's own optimal solution identified during the iteration (the "individual extreme value") and the optimal solution discovered by all particles in the population during the iteration (the "global extreme value"). Each particle has memory and only remembers two values.

The process of the PSO algorithm is as follows.

1) Initialize the particle swarm, including the group size *N*, the position x_i of each particle, and the velocity v_i.

2) Calculate the fitness value fit [i] of each particle.

3) For each particle, compare the fitness value fit [i] with the individual extreme value pbest (i). If fit [i] < pbest (i), then replace pbest (i) with fit [i].

4) For each particle, compare the fitness value fit [i] with the global extremum gbest. If fit [i] < gbest, then replace gbest with fit [i].

5) Iteratively update the particle's velocity v_i and position x_i.

6) Process boundary conditions.

7) Determine whether the termination condition of the algorithm is satisfied: if yes, the algorithm is terminated and the optimization result is output. Otherwise, return to step 2.

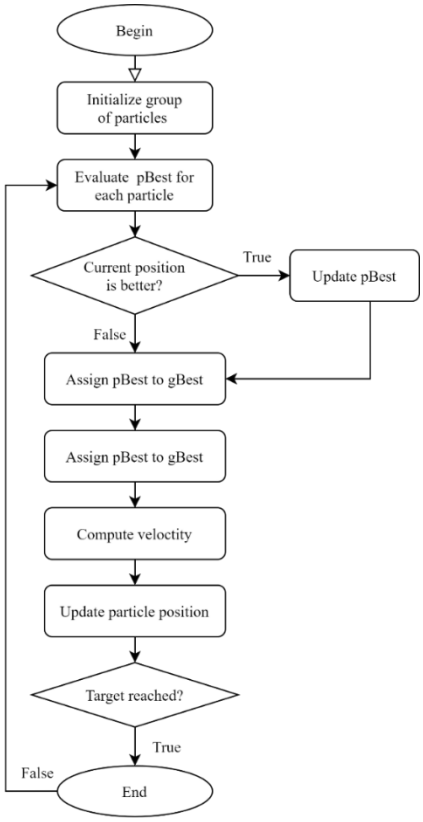

Fig. 2 PSO algorithm

The main parameters of the PSO algorithm include the inertia weight ω and two learning factors, $c1$ and $c2$. Effective adjustment of these parameters, either statically or dynamically, can significantly enhance the optimization efficiency of the PSO algorithm and its capability to escape local optimal solutions.

The inertia weight ω is crucial in influencing the particle's tendency to maintain its current speed (or "inertia") towards its previous trajectory. Modifying the inertial weight can balance the particle's ability to explore the unknown solution space with its ability to approach the optimal solution. Specifically, a larger inertia weight ω encourages global searching, enhancing the particle's exploration of the solution space. Conversely, a smaller inertia weight ω promotes local searching, strengthening the particle's ability to approach the optimal solution.

To address the nonlinear integer programming with relatively low spatial dimensions, a linear decreasing dynamic adjustment strategy was employed in this study:

$$\omega_k = \frac{\omega_0 (\omega_0 - \omega_{end}) (T_{\max} - k)}{T_{\max}} \quad (12)$$

where ω_0 is the initial weight, ω_{end} is the weight at the maximum number of iterations, k is the current number of iterations, and *Tmax* is the maximum number of iterations. This strategy begins with a large inertia weight for global searching and gradually decreases it, favoring local searching in the process. This strategy has proven effective in many cases.

Variables c1 and c2 represent the individual and group learning factors, respectively; c1 is the self-learning factor (where particles learn from their own experience) and c2 is the social-learning factor (where particles learn from group experience). Initially, c1 is greater than c2 to encourage exploration. Later, c2 becomes greater than c1 to utilize obtained information more effectively. This can be achieved by linearly decreasing c1 and linearly increasing c2.

For c1 (self-learning factor):

$$c1 = c1_0 - (c1_0 - c1_{end}) * (k/\mathrm{Tmax}) \quad (13)$$

and for c2 (social-learning factor):

$$c2 = c2_0 + (c2_{end} - c2_0) * (k/\mathrm{Tmax}), \quad (14)$$

where $c1_0$ and $c2_0$ are the values of c1 and c2 at the beginning of the search, and $c1_{end}$ and $c2_{end}$ are the values of c1 and c2 at the end of the search; k is the current number of iterations, and Tmax is the total number of iterations. This strategy can ensure that the particles have sufficient global search ability in the early stages of the search, and local search ability in the later stages.

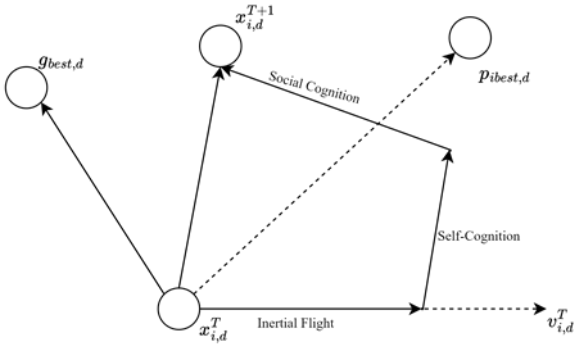

Fig. 3 Enhanced PSO algorithm (2)

The optimal solution as per the enhanced PSO algorithm is: $\begin{cases} n_A = 1 \\ n_B = 2. \\ n_C = 2 \end{cases}$

III. Environmental Profile Similarity of Original, Spare Samples

In this study, we assumed that the original and spare part samples originate from the same production batch and share identical production dates and processes. The original parts undergo a duty period on the platform whereas the spare parts are stored in the warehouse under slightly different temperature and humidity conditions. Considering the temperature and humidity variations in the storage environments between the original and spare part samples, a DTW model was established to resolve the similarity function, quantify the specific differences, measure the similarity between the original and spare part samples, and enhance the sample evaluations.

This study addressed a practical scenario involving two sample types (original parts and spare parts) with the goal of analyzing their storage environments and evaluating their similarity under distinct coditions. The spare part samples, stored in a stable environment, experience minimal temperature and humidity fluctuations, In contrast, beyond storage, the original part samples are exposed to varying temperature conditions on duty. To comprehensively measure the differences between these two types of samples, we introduced a similarity function with clear physical significance and ease of solution.

DTW, recognized for ts effectiveness in measuring sequence similarity, is widely applied in various fields including speech recognition, pattern matching, and time series analysis. Particularly suited for processing time series data, DTW accommodates slight time offsets or stretches in data. This characteristic lends significant advantages in comparing the similarity between dual time series. The fundamental concept of DTW involves aligning two time series on a time axis through transformation, aiming to identify the optimal matching path. This path minimizes some distance measure (e.g., Euclidean distance) between the two series. By dynamically adjusting the correspondence between the two series, DTW minimizes the total distance and thus effectively handles nonlinear deformations like time scaling and translation.

To operate the DTW algorithm, it is first necessary to create a distance matrix of size n×m, where n and m are the lengths of the two respective time series (1 and 2). Each element (i, j) in the matrix represents the distance between the i_{th} element of series 1 and the j_{th} element of series 2. This distance can be defined as Euclidean or with other distance measures.

Next, from the upper left corner of the matrix, the cumulative distance of each cell is calculated in turn. The value of each cell is the sum of the distance of the current position and the minimum cumulative distance in the three cells on the left, upper, and upper left sides. Through dynamic programming, the entire matrix can be filled in this manner.

Finally, by backtracking the distance matrix, the minimum cumulative distance path from the lower right corner to the upper left corner can be identified. This path serves to map a time series to the optimal correspondence of another time series, ultimately yielding the optimal path.

The details of DTW algorithm are as follows.

1. Define the cost matrix:

$$Dist(X_i, Y_j) = Dist(X_i, Y_j) + min\left[Dist(X_{i-1}, Y_{j-1}), Dist(X_{i-1}, Y_j), Dist(X_i, Y_{j-1})\right], \tag{15}$$

where $1 \le i \le N, 1 \le j \le M$.

2. Compare the two series and fill the matrix with the minimum European distance to determine the distance after dynamic time distortion: $Dist(X, Y) = Dist(X_N, Y_M)$.

(16)

3. The minimum distance path after setting the twisted time position is : $W = w_1, w_2, \cdots, w_K$, where $\max(N, M) \le K \le N + M w_k = (i, j), w_{k+1} = \left(\acute{i}, \acute{j}\right), i \le \acute{i} \le i + 1, j \le \acute{j} \le j + 1.$

(17)

4. Substitute the upper formula into series 1: $Dist(X, Y) = Dist(W) = \sum_{k=1}^{K} Dist(w_k)$.

(18)

5. Backtrack to determine the optimal path:

$$\begin{aligned} W_k &= (i,j) \\ w_{k-1} &= \operatorname{argmin} Dist(i-1,j), Dist(i,j-1), Dist(i-1,j-1) \end{aligned}. \tag{19}$$

In this study, we used DTW as the main tool to quantify the similarity between original and spare part samples under different storage conditions. As discussed above, DTW is unique in its flexibility and robustness. It can effectively handle nonlinear deformations of time series data, including time scaling, translation, and others, lending it a high degree of accuracy and stability in various applications. Even if there is a slight offset or stretch between the two time series, DTW can successfully identify the optimal matching path between them.

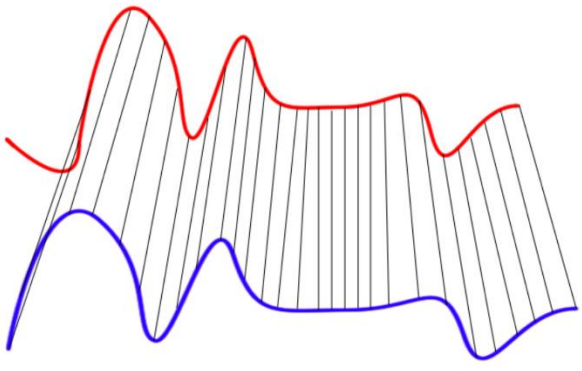

Fig. 4 Schematic diagram of dynamic time warping

We used DTW to calculate the similarity between the original and spare part samples. To measure this similarity as scientifically as possible and to ensure unity with other similarities, we introduced the "relative dynamic time warping ratio" R_{DTW}, which effectively measures the similarity between two time series.

$$R_{DTW} = 1 - \frac{\log(1 + DTW_{now})}{\log(1 + DTW_{\max})} \quad (20)$$

In Eq. (20), the logarithmic function log (1+x) facilitates normalization. The term 1 prevents errors when DTW_{now} = 0 or $DTW_{max} = 0$ while the log function measures the similarity. When the value of DTW_{now} is large, the increased normalized value is small; this minimizes the influence of large DTW distances. For small DTW_{now} values, the increased normalization value is relatively large, which emphasizes the influence of small DTW distances. The calculated value was divided by the maximum possible value to obtain the relative proportion.

The advantages of this method can be summarized as follows.

1. Strong interpretability: The value of R_{DTW} ranges between 0 and 1, which makes the results readily interpretable. A closer score to 0 indicates lower similarity between the two time series and a score closer to 1 implies they are more similar.

2. Robustness: By comparing the DTW distance with the maximum possible DTW distance, R_{DTW} minimizes the influence of different data ranges or scales, making the similarity score more robust.

3. Easy to operate: The calculation process of R_{DTW} is simple, intuitive, and does not require complex parameter adjustments. It was easily applied to the multi-year accumulated temperature and humidity data utilized in this study.

The R_{DTW} of the original and spare part samples was determined to be 0.9043, indicating a very high level of similarity between them. When confronted with a situation where the number of original parts is limited, yet a substantial sample size is required for experimentation, considering the two sample types as adhering to the same distribution would be a reasonable approach. Utilizing spare parts to supplement the original parts in the test appears to be a sensible sample enhancement method.

Given that the original and spare part samples belong to the same type of equipment, and exhibit high similarity despite their differing storage conditions, spare parts can be treated as an unbiased estimate of the original parts. The confidence interval is:

$$[\hat{\mu} - Z_{\alpha/2} * \frac{\hat{\sigma}}{\sqrt{n}}, \hat{\mu} + Z_{\alpha/2} * \frac{\hat{\sigma}}{\sqrt{n}}] \quad (21)$$

where $Z_{\alpha/2}$ is the $\alpha/2$ quantile of the standard normal distribution. For the 95% confidence level, $Z_{\alpha/2} \approx 1.96$. In this study, the test sample weight score $C = (n_{Original} + R_{DTW} * n_{Spare})/(n_{Original} + n_{Spare})$ was defined to calculate the influence of adding spare part samples to the original sample set. The results are detailed below.

Table 4 Score, confidence interval of sample weight after spare sample test

Number of spare part samples	Number of original part samples	Sample weight score	Confidence interval
0	5	1.0	$[\hat{\mu} - 1.96 * \hat{\sigma}\sqrt{5}, \hat{\mu} + 1.96 * \hat{\sigma}\sqrt{5}]$
1	5	0.96	$[\hat{\mu} - 1.96 * \hat{\sigma}\sqrt{6}, \hat{\mu} + 1.96 * \hat{\sigma}\sqrt{6}]$
2	5	0.93	$[\hat{\mu} - 1.96 * \hat{\sigma}\sqrt{7}, \hat{\mu} + 1.96 * \hat{\sigma}\sqrt{7}]$
3	5	0.91	$[\hat{\mu} - 1.96 * \hat{\sigma}\sqrt{8}, \hat{\mu} + 1.96 * \hat{\sigma}\sqrt{8}]$

4	5	0.89	$[\hat{\mu} - 1.96 * \hat{\sigma}\sqrt{9}, \hat{\mu} + 1.96 * \hat{\sigma}\sqrt{9}]$
5	5	0.87	$[\hat{\mu} - 1.96 * \hat{\sigma}\sqrt{10}, \hat{\mu} + 1.96 * \hat{\sigma}\sqrt{10}]$

Table 4 reveals that even with an increased number of spare part samples, the overall experiment's weight score did not significantly decrease. This suggests that incorporating spare part samples into the experiment did not adversely impact the results of the original experiment. Fisher's exact test was used to further demonstrate the influence of adding spare part samples to the original samples in this experiment.

Fisher's exact test assesses the correlation between two variables based on is a 2x2 contingency table, providing an output in terms of odds ratio and an exact p-value.

1. The odds ratio represent the ratio of the probability of an event occurring to that of the event not occurring. In Fisher's exact test, the odds ratio is the ratio between the probability of events occurring under one condition and that under another condition. When comparing the performance of spare part samples and original part samples, the odds ratio was defined as the ratio of the probability of spare parts passing the test to the probability of the original parts passing the test. An odds ratio is greater than 1 indicates a higher pass rate for spare parts than for original parts; a ratio less than 1 suggests a lower pass rate for spare parts compared to original parts.

2. The p-value is the probability of observing the current or more extreme results under the premise that the null hypothesis is true (in this case, assuming the pass rates of the spare part samples and the original part samples are the same). Small p-values (usually <0.05) indicate a significant difference between the observed results and the null hypothesis. In this study, p-values less than 0.05 were considered to indicate significant differences between the pass rates of spare and original part samples.

Assuming a specified number of original part samples and varying results for pass/fail inspections, the test outcomes are listed in Table 5.

Table 5 Significance of passing rates on original/spare part tests

Test results for original part samples		Test results for spare part samples		Inspection results	
Passed	Not passed	Passed	Not passed	Odds ratio	p_value
5	0	10	0	-	1
		9	1	-	1
		8	2	-	0.523
		7	3	-	0.505
4	1	10	0	0	0.333
		9	1	0.444	1
		8	2	1	1
		7	3	1.714	1
3	2	10	0	0	0.095
		9	1	0.167	0.242
		8	2	0.375	0.56
		7	3	0.643	1
2	3	10	0	0	0.022
		9	1	0.074	0.077
		8	2	0.167	0.251
		7	3	0.286	0.329

In scenarios where all five original part samples passed the test and only 10 spare part samples passed the test, the odds ratio could not be calculated due to a denominator of 0; the p-value was 1. This implies that, under the null hypothesis (i.e., the pass rates of original and spare part samples are the same), the likelihood of observing the current or more extreme results is very high. Consequently, no significant difference in the pass rates between the original and spare part samples could be concluded.

In cases where four original part samples passed the test, one failed, and only 10 spare part samples passed the test, the odds ratio was 0 and the p-value was 0.333. Again, no significant difference in the pass rate between the original and spare part samples could be concluded.

When three original part samples pass the test, two failed, and 10 spare part samples passed the test, the odds ratio was 0 and the p-value was 0.095. Although the p-value is small, it still exceeds 0.05 and thus provides sufficient evidence to reject the null hypothesis, indicating a significant difference in the pass rate between the original and spare part samples.

When two original part samples passed the test, three failed, and 10 spare part samples passed the test, the odds ratio was 0 and the p-value was 0.022. This p-value is less than 0.05, rejecting the null hypothesis; again, there is a significant difference in the pass rate between the original and spare part samples in this case.

Evidently, in most cases, no significant difference in pass rates between the original and spare part samples can be concluded. Only in one case was it possible to infer a significant difference in pass rate (when the pass rate of spare parts was 100% and the pass rate of original parts was 40% or lower). Generally, when the pass rate of spare part samples was higher than or equal to 70%, we did not have sufficient evidence to suggest a significant difference in pass rate between the original part samples and spare part samples.

IV. Similarity and Inheritance Factors of New and Old Product Models

As an index in information theory measuring the dependency between two random variables, mutual information (MI) measures the degree of information sharing between them – essentially, how much additional information one random variable can provide to another through the observed values of the former.

For two discrete random variables X and Y, their MI, denoted as $MI(X,Y)$, is defined as follows:

$$MI(X,Y)=\sum_{x\in X}\sum_{y\in Y}p(x,y)\log\left(\frac{p(x,y)}{p(x)p(y)}\right) \tag{22}$$

where p (x, y) is the joint probability distribution function of X and Y, and p (x) and p (y) are the marginal probability distribution functions of X and Y, respectively.

The joint entropy H (X, Y) is expressed as:

$$H(X,Y)=-\sum_{y\in Y}\sum_{x\in X}p(x,y)\log(p(x,y)), \tag{23}$$

while the entropy of (X), (H(X)) and the entropy of (Y), (H(Y)) is:

$$H(X)=-\sum_{x\in X}p(x)\log(p(x)), \tag{24}$$

$$H(Y)=-\sum_{y\in Y}p(y)\log(p(y)). \tag{25}$$

In the above equations, the joint entropy (H(X,Y)) is consistently greater than or equal to the sum of the entropy (H(X)) of (X) and (H(Y)) of (Y). MI can be defined as the sum of the entropy of (X) and the entropy of (Y) minus their joint entropy, that is:

$$I(X;Y) = H(X) + H(Y) - H(X,Y) .$$

(26)

Average MI I (X; y) is stable, so it becomes a definite metric. The unit of MI is defined as a "bit" when using 2-based logarithms. The size of the MI reflects the degree of correlation between the two variables: a greater value indicates a stronger correlation, and vice versa. In the case where the two variables are completely independent, the MI value is 0. If X is a deterministic function of Y, and Y is also a deterministic function of X, then all information is shared by both: knowing X determines the value of Y, and vice versa. In this case, the value of MI is equal to the entropy of Y (or X), representing the uncertainty contained in Y (or X). Simultaneously, this MI value is equal to the entropies of X and Y.

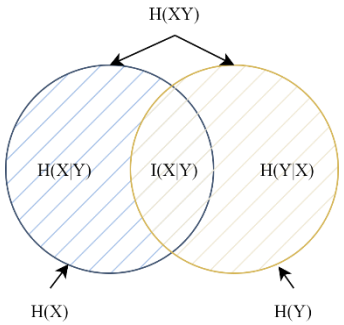

Fig. 5 Mutual information

In the field of equipment research, experiments involving new models often entail significant cost investments, leading to strict limitations on the scale of sampling. The constrained sample size can impact the confidence level of experimental results. In such scenarios, considering the MI between new and old models becomes imperative. In practice, by quantitatively measuring MI, it becomes possible to scientifically compare the two equipment models, evaluate the performance of new models despite limited resources, and eliminate the necessity for extensive sampling experimentation.

As an important index in information theory, MI serves not only to quantify the interdependence between two random variables but can also be applied to research scenarios such as ours for measuring the similarity between different product models. Calculating the MI between new and old models allowed us to quantitatively assess the shared information between them, offering strong support for subsequent experimental design and data analysis.

In the realm of reliability engineering, there is often insufficient field test data for new products, while similar old products gain sufficient reliability information as they mature. If it can be determined that the fault information of an old product is compatible with that of its newer version, the information of the old product can typically be considered equivalent ot the new product for evaluating its reliability. To simultaneously capture the inheritance and difference of information, the concept of an "inheritance factor" was introduced in this study when processing prior information. The inheritance factor reflects the similarity between new and old products and significantly influences on the results of final reliability evaluations. By adjusting the inheritance factors, it is possible to control the influence of old product information on the evaluation of new products while enhancing the accuracy and reliability of the evaluation results.

Building upon the data we gathered in the first stages of this study, the calculation method for inheritance factor ρ was adjusted as follows:

$$\rho = \frac{e^{MI} - 1}{e - 1}$$

(27)

where *MI* is the value of MI between new and old models, which is easily obtained from the above formula as $\rho \in [0,1]$. When new and old models are more similar (i.e., have *MI* close to 1), the inheritance factor ρ is closer to 1; conversely, it is closer to 0.

Furthermore, *MI* is always non-negative, so the value range of ρ is between [0,1]. The inheritance factor can be intuitively interpreted as the similarity between old and new products: 0 indicates they are completely dissimilar and 1 means they are completely similar.

This formula constitutes a smooth, continuous function. The introduction of *e* as the exponential function, defined by the base number, adeptly captures the continuous and uniform change trend. This variable has been extensively employed in relevant theorems of information theory, such as those describing the nature of MI. The use of *e* aligns with pertinent conclusions under information theory. As *MI* increases, ρ smoothly increases without apparent steps. This reflects a gradual change in the similarity between old and new products, where even minor changes in *MI* lead to subtle changes in ρ. Consequently, this inheritance factor accurately reflects the similarity between new and old products.

In addition, the formula of ρ reflects inheritance. As a method for measuring the degree of interdependence between two random variables, a larger *MI* value indicates stronger correlation between them. Therefore, when old and new products have higher MI, the corresponding ρ value will also be larger, indicating that the new product retains more characteristics of the old one.

Another advantage of this formula is that when *MI* is 0, ρ will also be 0. When *MI* approaches the joint entropy of the new and old models, ρ will approach 1. This implies that when the new product is entirely unrelated to the old product, the value of the inheritance factor is 0, and the information of the old product can be disregarded. When the new product is closely related to the old product, the value of the inheritance factor is close to 1, and the new product can be considered to almost completely inheri the information of the old product. These phenomena align with our intuitive understanding of inheritance factors, adding to the formula's credibility.

For each experimental scenario, the following steps were repeated to enhance the confidence level after mixing the samples.

1. Mix the corresponding number of samples B with samples A and calculate the mutual information of the mixed sample.

2. Multiply the temperature and humidity values of the old sample in the MI be multiplied by the inheritance factor.

3. Perform a Wilcoxon-Mann-Whitney rank sum test to determine the corresponding confidence level.

The Wilcoxon-Mann-Whitney rank sum test, commonly known as the Mann-Whitney U test, is a non-parametric statistical hypothetical testing method for determining whether significant differences exist between two independent samples. It is particularly suitable for cases where the assumptions of normality and homogeneity of variance required for parameter testing cannot be satisfied. The test evaluates the null hypothesis H0, which posits that the probability that the observation value of one group (A) being greater than that of the other group (B) is equal to the probability of it being smaller. The alternative hypothesis H1 contends that the probability of the observation values of one group being greater than those of the other group is different. The steps to this process are as follows.

1. Merge the data from the two groups and sort them in ascending order, assigning a rank to each observation value regardless of its group of origin.

2. Calculate the rank sum of each group.

3. Calculate calculatethe U statistics of the inspection as:

$U = n_x n_y + \frac{n_x(n_x+1)}{2} - R_x$, where n_x and n_y are the numbers of two sets of observations, respectively, and the statistic represents the smaller one of the two rank sums.

4. Compare the obtained U statistics with the critical values corresponding to the expected saliency level and degrees of freedom in the Mann-Whitney U table. If the obtained U statistic is less than or equal to the critical value, the null hypothesis is rejected.

If the null hypothesis is rejected, then there is a significant difference between the two groups in terms of the variables under analysis. If the null hypothesis is not rejected, then there is insufficient evidence of significant differences.

Table 6 Influence of combined similar models on p-values of new samples

Similar model sample/new model sample	4	5	6
1	0.1571	0.1433	0.1332
2	0.3543	0.1459	0.1825
3	0.0179	0.1014	0.0743
4	0.0077	0.0049	0.0331
5	0.0041	0.0017	0.0169
6	0.0022	0.0014	0.0088
7	0.0016	0.0012	0.0056
8	0.0013	0.0011	0.0024

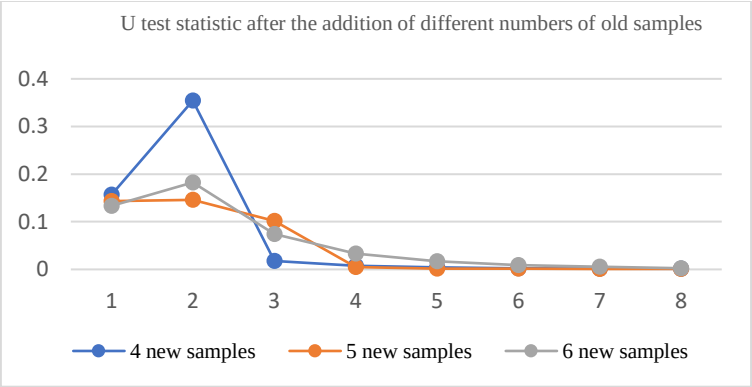

Fig. 6 U test statistics after addition of old samples

The chart above provides a detailed description of how the p-value in the hypothesis test was influenced by varying numbers of new samples when different quantities of old samples were introduced. Each row illustrates the outcomes when a specific number of old samples were added, while each column depicts the outcomes with a specific number of new samples.

Consider the scenario of 4 new samples as an example. When 1 old sample was added, the p-value was 0.1571. However, when 2 old samples were added, the p-value increased significantly to 0.3543. Notably, as the number of old samples continued to increase, the p-value began to decline gradually. This decline became evident when the number of old samples reached 3, resulting in a p-value of 0.0179. This trend persisted with further increases in the number of old samples.

Similar trends were observed when there were 5 or 6 new samples. Adding 1 or 2 old samples led to an increase in the p-value, yet as the addition of old samples continued, the confidence level trended downward. The overall trend, as evident from the chart, indicated that an increase in the number of old samples (especially beyond 2) caused the p-value of the experiment to consistently decline, irrespective of the number of new samples. This implies that while the addition of a small number of old samples (1-2) can significantly enhance test confidence, further increases in the number of old samples gradually diminishes or even reverses this effect.

V. Conclusion

In addressing concerns regarding the representativeness of experimental sample selection in current storage life extension projects, as well as the low confidence associated with conclusions drawn from small sample sizes, we refined a sample selection method in this study for equipment life extension tests and enhanced test confidence in scenarios involving limited samples. A novel and scientifically grounded approach to subsample selection was established. Building upon an authoritative equipment quality monitoring standard, we meticulously refined the secondary indexes of the equipment technical status evaluation system. The comprehensive weighting method, employing neural networks and social networks, was applied to assess the secondary indexes. An enhanced PSO algorithm was utilized to address the challenges posed by small sample models in accelerated life tests, facilitating the selection of representative sampes for experimentation.

Recognizing the limitations of small sample test conclusions in terms of the necessary confidence levels under classical mathematical reliability sampling theory, we developed a method based on the DTW algorithm and MI method. The proposed method combines test information derived from spare part samples with information from similar models, effectively expanding the sample size in a rational manner. This method demonstrated the potential to significantly enhance confidence levels in equipment life extension tests.

References

[1] Jun, L., Ling, M., Lixin, Z., & Chunhui, W. (2014, August). A concept for PHM system for storage and life extension of tactical missile. In 2014 Prognostics and System Health Management Conference (PHM-2014 Hunan) (pp. 689-694). IEEE.

[2] Gao, J., Huang, D. P., & Li, X. B. (2015). Overall Solution of Comprehensive Evaluation for Missile Storage Life. Applied Mechanics and Materials, 724, 307-311.

[3] Ito, K., & Nakagawa, T. (2000). Optimal inspection policies for a storage system with degradation at periodic tests. Mathematical and Computer Modelling, 31(10-12), 191-195.

[4] Pant, S., Kumar, A., Ram, M., Klochkov, Y., & Sharma, H. K. (2022). Consistency indices in analytic hierarchy process: a review. Mathematics, 10(8), 1206.

[5] Saaty, R. W. (1987). The analytic hierarchy process—what it is and how it is used. Mathematical modelling, 9(3-5), 161-176.

[6] Golden, B. L., Wasil, E. A., & Harker, P. T. (1989). The analytic hierarchy process. Applications and Studies, Berlin, Heidelberg, 2(1), 1-273.

[7] Mishra, S. P., Sarkar, U., Taraphder, S., Datta, S., Swain, D., Saikhom, R., ... & Laishram, M. (2017). Multivariate statistical data analysis-principal component analysis (PCA). International Journal of Livestock Research, 7(5), 60-78.

[8] Paul, L. C., Suman, A. A., & Sultan, N. (2013). Methodological analysis of principal component analysis (PCA) method. International Journal of Computational Engineering & Management, 16(2), 32-38.

[9] Zhu, Y., Tian, D., & Yan, F. (2020). Effectiveness of entropy weight method in decision-making. Mathematical Problems in Engineering, 2020, 1-5.

[10] Shen, Y., Chen, D., Zhang, M., & Zuo, T. (2022). Fuzzy comprehensive safety evaluation of pipeline disaster in China-Russia crude oil permafrost region based on improved analytic hierarchy process-entropy weight method. Advances in Materials Science and Engineering, 2022.

[11] Wasserman, S., & Faust, K. (1994). Social network analysis: Methods and applications.

[12] Oliveira, M., & Gama, J. (2012). An overview of social network analysis. Wiley Interdisciplinary Reviews: Data Mining and Knowledge Discovery, 2(2), 99-115.

[13] Zhu, D., Wang, H., Wang, R., Duan, J., & Bai, J. (2022). Identification of key nodes in a power grid based on modified PageRank algorithm. Energies, 15(3), 797.

[14] Rogers, I. (2002). The Google Pagerank algorithm and how it works.

[15] Chin, W. C. B., & Wen, T. H. (2015). Geographically modified PageRank algorithms: Identifying the spatial concentration of human movement in a geospatial network. PloS one, 10(10), e0139509.

[16] Chen, H., Wang, S., & Wang, H. (2009, August). Particle swarm optimization based on genetic operators for nonlinear

integer programming. In 2009 International Conference on Intelligent Human-Machine Systems and Cybernetics (Vol. 1, pp. 431-433). IEEE.

[17] Sahoo, L., Banerjee, A., Bhunia, A. K., & Chattopadhyay, S. (2014). An efficient GA–PSO approach for solving mixed-integer nonlinear programming problem in reliability optimization. Swarm and Evolutionary Computation, 19, 43-51.

[18] Sun, R., Yang, Z., & Hong, Q. (2018). A PSO-Based Integer Programming Solution to Impulsive-Correction Projectile Systems. Innovative Techniques and Applications of Modelling, Identification and Control: Selected and Expanded Reports from ICMIC'17, 13-30.

[19] Cuturi, M., & Blondel, M. (2017, July). Soft-dtw: a differentiable loss function for time-series. In International conference on machine learning (pp. 894-903). PMLR.

[20] Guo, F., Zou, F., Luo, S., Liao, L., Wu, J., Yu, X., & Zhang, C. (2022). The fast detection of abnormal ETC data based on an improved DTW algorithm. Electronics, 11(13), 1981.

[21] Paninski, L. (2003). Estimation of entropy and mutual information. Neural computation, 15(6), 1191-1253.

[22] Bachman, P., Hjelm, R. D., & Buchwalter, W. (2019). Learning representations by maximizing mutual information across views. Advances in neural information processing systems, 32.